



## Chemical variations and origin of tourmalines in Laleh Zar granite of Kerman (Southeast Iran)

Sadaf Ahmadi, Zahra Tahmasbi, Ahmad Ahmadi Khalaji\*, Farhad Zal

Department of Geology, Faculty of Sciences, Lorestan University, Khorramabad, Iran

### ARTICLE INFO

Submitted: January 2019

Accepted: February 2019

Available on line: March 2019

\* Corresponding author:

ahmadikhaj.a@lu.ac.ir

DOI: 10.2451/2019PM844

How to cite this article:

Ahmadi S. et al. (2019)

Period. Mineral. 88, 117-129

### ABSTRACT

Tourmalines in the Laleh Zar granite of Kerman are found in a variety of forms including: (1) nodule tourmaline; (2) radial tourmaline, and (3) vein tourmaline. Electron microprobe analyses of the tourmalines have revealed a wide compositional variation between schorl and dravite end members. These tourmalines belong to alkali group. Mg/(Mg+Fe) ratios for radial, nodule, and vein tourmalines range from 0.37 to 0.53, 0.36 to 0.59, and 0.30 to 0.46, respectively; and Ca/(Ca+Na) ratios for radial, nodule, and vein range from 0.17 to 0.35, 0.16 to 0.38, and 0.09 to 0.35, respectively. All tourmalines have Al content lower than 6 atoms per formula unit compared with the theoretical value of 6 in ideal schorl and dravite, showing the studied tourmalines do not contain enough Al to fill the Z-site. The occurrence of X-vacancy and Al at the Y site of the three types of tourmaline are negligible. Nodule tourmalines have chemical and color-zoning patterns, whereas radial and vein tourmalines only have chemical-zoning patterns including significant fluctuations in Al, Fe, Mg, Na, Ca, and Ti. Based on petrographic and chemical properties of tourmalines, vein tourmaline has been formed during a transition from magmatic to hydrothermal processes and radial tourmaline has been formed by mixing magmatic-hydrothermal fluids with an external fluid rich in Ca and Mg, whereas nodule tourmaline is probably the result of post-magmatic hydrothermal environment, through the influence of an external fluid that could for example have come from the wall rocks to the nodule.

Keywords: Nodule tourmaline; radial tourmaline; vein tourmaline; schorl; dravite; Laleh Zar granite.

### INTRODUCTION

Tourmaline is a complex borosilicate mineral supergroup that has a general structural formula of  $XY_3Z_6[T_6O_{18}](BO_3)_3V_3W$ , where  $X=Na, Ca, K,$  and  $\square$ ,  $Y=Li^{1+}, Mg^{2+}, Fe^{2+}, Mn^{2+}, Al^{3+}, Cr^{3+}, V^{3+}$  and  $Ti^{4+}$ ,  $Z=Al^{3+}, Fe^{3+}, V^{3+}, Cr^{3+}, Mg^{2+}$  and  $Fe^{2+}$ ,  $T=Si, Al,$  and  $B$ ,  $V=OH, O,$  and  $W=OH, O,$  and  $F$  (Hawthorne and Henry, 1999; Bosi, 2018). Tourmaline could be found in a variety of geological environments and is a common accessory mineral in granitic pegmatites, low- to high-grade metamorphic rocks, and clastic sedimentary rocks. Tourmaline complex composition reflects the changes

in its chemical and physical environments, such that tourmaline chemistry can reflect the diverse compositions of both host rock and hydrothermal fluids (Henry and Guidotti, 1985). Moreover, the composition of tourmaline provides information about mineralizing conditions, fluid flow, and possible sources of constituents in hydrothermal systems, e.g., in magmatic-hydrothermal systems (Pirajno and Smithies, 1992), that originated from external fluids (Palmer and Slack, 1989 and Xavier et al., 2008). The conditions for formation of tourmaline have always been discussed; for example, common hypotheses about the formation of tourmaline nodules include the following: (1)

from post-magmatic replacement related to hydrothermal alteration of previously crystallized granite by boron-rich fluids which infiltrate through micro-fractures and diffuse along grain boundaries (Rozendaal and Bruwer, 1995). (2) as magmatic-hydrothermal properties related to the exsolution, separation, and entrapment of immiscible aqueous boron-rich fluids from coexisting granitic magma (Samson and Sinclair, 1992; Trumbull et al., 2008; Balen and Broska, 2011; Yang and Jiang, 2012); (3) crystallized directly from a B-rich granitic melt (Perugini and Poli, 2007). There are several distinct morphology types of tourmaline in laleh Zar granite such as nodule tourmaline, tourmaline-enriched veins, and radial tourmaline. This paper focuses on the details of mineral chemistry and chemical zoning in the three types of tourmaline from laleh Zar granite in order to determine the conditions of their formation.

#### LOCAL GEOLOGY

Laleh Zar granite is located in the Southeast of Kerman of Iran and is a part of the Urumieh-Dokhtar magmatic Arc (UDMA). This intrusion is located in the regional geological map of Baft with 1:100,000 scale (Figure 1; Dimitrijevic, 1973). The UDMA is a recent active continental margin in Central Iran. Rifting in the Red Sea-Gulf of Aden region (Guiraud and Bosworth, 1997) led to the Neotethyan Oceanic closure and collision between Arabian and Iranian plates during the Late Oligocene (Mohajjel et al., 2003; McClay et al., 2004; Agard et al., 2005). During the middle-late Neogene, the subduction of Neotethyan under the Iranian plate led to a new plate tectonic configuration; in this period, the changes in the convergence rate between Arabian and Iranian plates led to felsic magmatism (Shafiei et al., 2009) with 450 km in length and 60-80 km in width, Southeastern part of Central Iran in Kerman, the so-called Dehaj-Sarduieh subdivision or Kerman Magmatic Arc (KMA; Shafiei et al., 2009), is comprised of Miocene intrusive rocks and Eocene volcano-sedimentary rocks, which are intruded by the Jebal Barez-type intrusive rocks (Dimitrijevic, 1973). The study area is in eastern part of Dehaj-Sarduieh volcanic belt, which is a part of the south section of UDMA (Dimitrijevic, 1973). The Kerman magmatic belt (KMB) is comprised of voluminous intrusive and extrusive rocks which are mostly calc-alkaline in nature. Generally, the KMB contains two different types of igneous rocks: (1) barren late Eocene-Oligocene granitoid and subvolcanic rocks (the Jebal Barez-type rocks) and (2) fertile mid-late Miocene intrusive bodies (Kuh Panj-type rocks). Most porphyry Cu-Au mineralizations are related to the emplacement of mid-late Miocene (Kuh Panj) granitoids, whereas most late Eocene-Oligocene (Jebel Barez) intrusions are barren of

Au-Cu mineralization (e.g., Dimitrijevic, 1973; Shafiei et al., 2008). The formation of adakitic and calc-alkaline rocks in KMB are attributed to three magmatic pulses in the Tertiary: (1) Eocene-Oligocene (Ahmadian et al., 2009), (2) Mid-Late Oligocene (Kirkham and Dunne, 2000; McInnes et al., 2005); and (3) Mid-Late Miocene (Razique et al., 2007; Richards, 2012). Most authors believe that adakitic magmatism has occurred during Miocene (e.g. Mc. Innes et al., 2005; Shafiei et al., 2009; Hou et al., 2011; Richards, 2012). These rocks are often exposed in the NE and central part of the RLMC. In terms of composition, these rocks vary from andesite to rhyolite without any mafic counterparts. Compositions of these rocks in Kerman region commonly vary from andesite to rhyolite without any mafic unit (Dimitrijevic, 1973; Hassanzadeh, 1993) and they have the characteristics of adakite rocks (Shafiei et al., 2009). Laleh Zar and Koh Shah granitoides are the most important of granitoid masses in this area.

#### ANALYTICAL METHODS

About 50 polished thin sections were prepared from tourmaline samples of Laleh Zar granite. After the tourmaline petrography study, 12 polished thin sections (including four nodule tourmaline samples, four radial tourmaline samples, and four vein tourmaline samples) were selected to determine the chemical composition of tourmaline by electron probe microanalysis (EPMA). 104 points of all the tourmalines were analyzed by this method. Composition of the major elements of the minerals was obtained using electron microprobe (JEOL JXA 8100) at the Institute of Geology and Geophysics, Chinese Academy of Sciences (IGGCAS), Beijing, China. Quantitative analyses were performed using wavelength-dispersive spectrometers (WDS) with an acceleration voltage of 15 kV, a beam current of 20 nA, a 5  $\mu$ m beam size. The elements were acquired using three crystals as follows: One LIFH for Cr, Mn, Fe, and Ni, one PETJ for K, Ca, and Ti and one TAP for Na, Mg, Al, and Si. The utilized standards were albite for Na, diopside for Si, Ca, and Mg, hematite for Fe, synthetic  $\text{Cr}_2\text{O}_3$  for Cr, synthetic  $\text{TiO}_2$  for Ti, orthoclase for K, synthetic  $\text{Al}_2\text{O}_3$  for Al, synthetic MnO for Mn, and synthetic NiO for Ni. The peak counting time was 20 s for all the elements and the background counting time was 10 s on the high- and low-energy background positions. All the data were corrected online using a modified ZAF (atomic number, absorption, fluorescence) correction procedure. Detection limits were in the range of 0.008-0.02 wt% ( $1\sigma$ ). The structural formula is based on a formalization scheme such that the proportion of Si equals 6 atoms per formula unit (apfu). Lithium was estimated by subtracting the sum of the Y-site cations from 3, i.e., assuming no vacancies

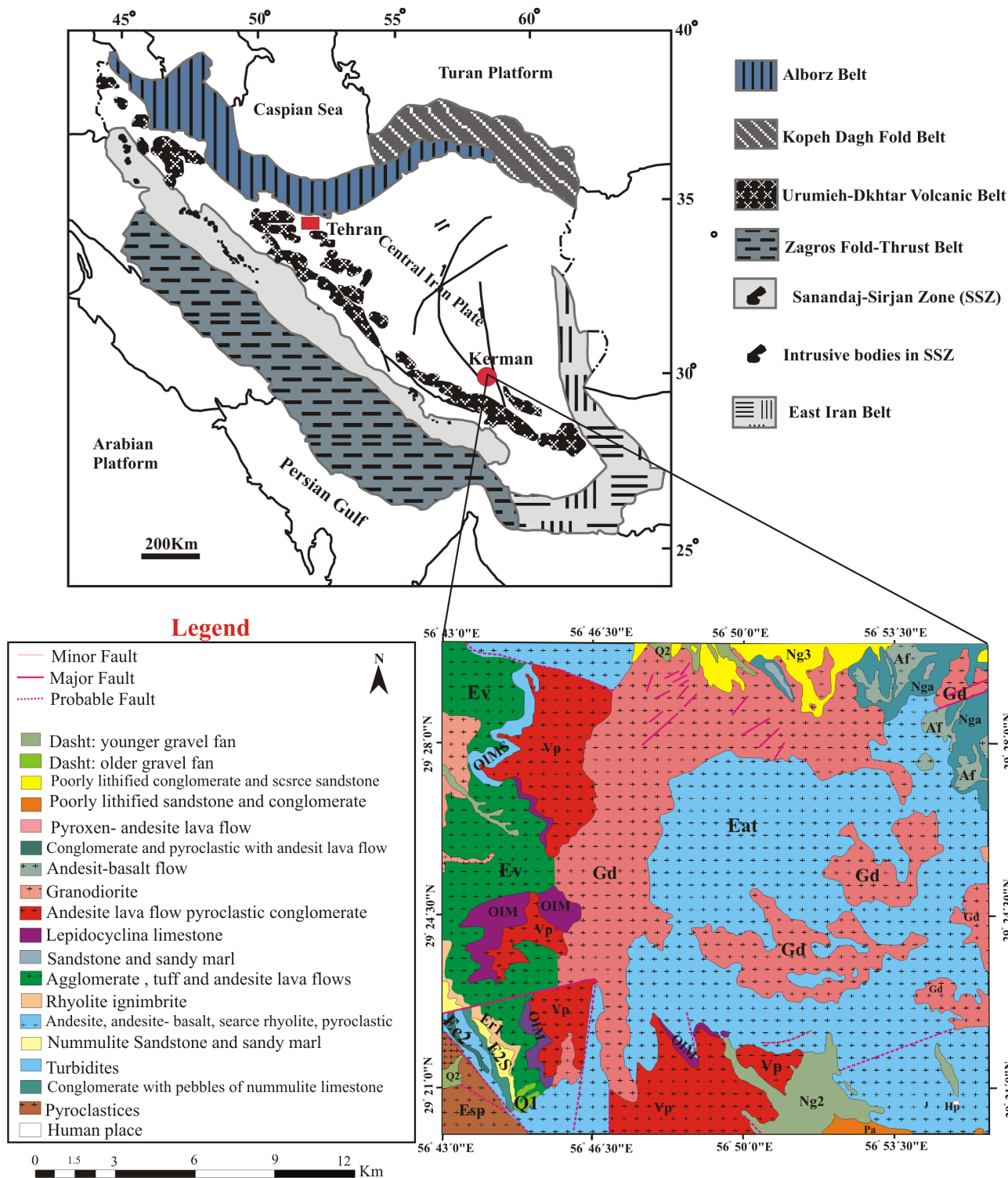


Figure 1. Geological sketch map of Iran and the study area based on the geological map 1:100,000 of Baft (Dimitrijevic, 1973).

at the octahedrally-coordinated sites (Henry and Dutrow, 1996). B<sub>2</sub>O<sub>3</sub> and H<sub>2</sub>O contents were calculated based on the stoichiometry for B=3 apfu and (OH+F)=4 apfu.

Representative analytical results are reported in Table 1. Full chemical data are available at the journal site as Supplemental Material.

Table 1. Data from EPMA of tourmaline.

	Radial N(34)			Vein N(32)			Nodule N(38)		
	min	max	average	min	max	average	min	max	average
SiO <sub>2</sub> (wt%)	34.30	37.70	36.20	34.20	36.60	35.50	34.30	37.20	35.60
TiO <sub>2</sub>	0.41	1.86	0.85	0.11	1.94	0.63	0.16	2.10	1.08
Al <sub>2</sub> O <sub>3</sub>	23.80	27.40	26.00	20.82	32.32	26.30	22.80	30.10	26.30
FeO	11.10	16.00	14.00	11.10	19.14	15.20	9.28	16.40	13.00
MnO	0.01	0.15	0.05	0.01	0.11	0.07	0.01	0.07	0.03
MgO	4.95	7.14	6.23	4.06	7.70	5.35	4.95	8.28	6.43
CaO	0.85	1.83	1.27	0.46	1.86	1.32	0.85	2.01	1.31
Na <sub>2</sub> O	1.89	2.51	2.23	1.88	2.51	2.21	1.79	2.63	2.20
K <sub>2</sub> O	0.02	0.13	0.05	0.02	0.06	0.04	0.02	0.13	0.06
H <sub>2</sub> O*	=	=	3.62	=	=	3.55	=	=	3.56
B <sub>2</sub> O <sub>3</sub> *	=	=	10.50	=	=	10.30	=	=	10.32
Li <sub>2</sub> O*	=	=	0.52	=	=	0.25	=	=	0.30
Si (apfu)	=	=	6	=	=	6	=	=	6
B	=	=	3	=	=	3	=	=	3
Z:Al	=	=	5.07	=	=	5.22	=	=	5.22
Mg	=	=	0.93	=	=	0.78	=	=	0.78
Y: Al	=	=	0.00	=	=	0.02	=	=	0.00
Mg	=	=	0.6	=	=	0.57	=	=	0.83
Fe	=	=	1.94	=	=	2.15	=	=	1.83
Ti	=	=	0.11	=	=	0.08	=	=	0.14
Mn	=	=	0.01	=	=	0.01	=	=	0.00
Li*	=	=	0.35	=	=	0.17	=	=	0.20
X: Ca	=	=	0.23	=	=	0.24	=	=	0.24
Na	=	=	0.72	=	=	0.72	=	=	0.72
K	=	=	0.01	=	=	0.01	=	=	0.01
Vacancy at X	=	=	0.05	=	=	0.03	=	=	0.03
(OH+F)	=	=	4	=	=	4	=	=	4
Mg/Mg+Fe	=	=	0.44	=	=	0.39	=	=	0.47
Ca/Ca+Na	=	=	0.24	=	=	0.25	=	=	0.25
FeO/FeO+MgO	=	=	0.69	=	=	0.74	=	=	0.67
R1=Na+Ca	=	=	0.94	=	=	0.96	=	=	0.95
R2=Fe(tot)+Mg+Mn	=	=	3.48	=	=	3.51	=	=	3.44
R3=Al+1.33Ti	=	=	5.21	=	=	5.35	=	=	5.40
Li*=9-(Z+Y) or 15-(T+Z+Y)									

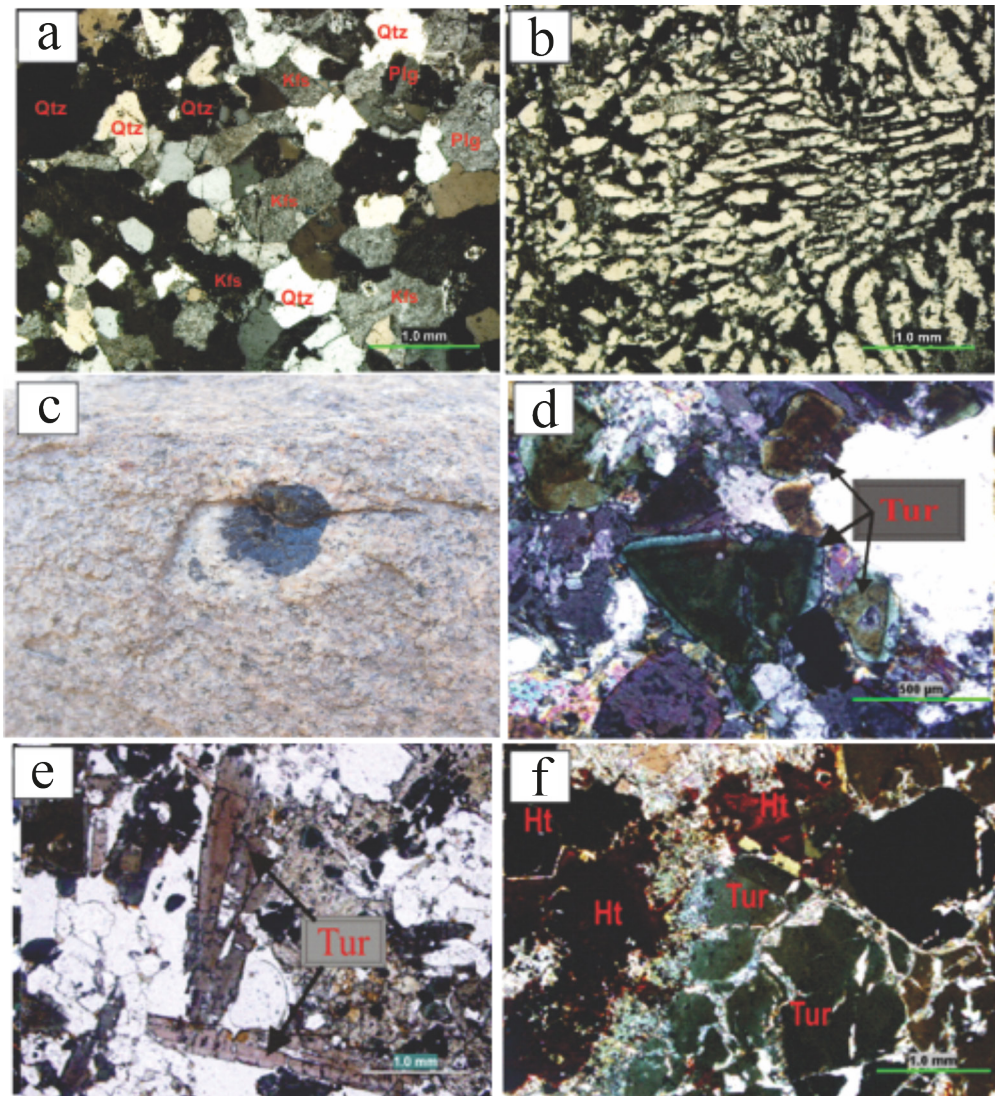


Figure 2. a) Granitic rocks with granular texture, plagioclase (Plg), quartz (Qtz) and alkali feldspar (Kfs) in light (XPL). b) Granophyric textures in granitic rocks. c) Tourmaline nodules in Laleh Zar granite. d) Triangular euhedral crystals with zoning color in nodule tourmaline. e) Columnar crystals in nodule tourmaline. f) Tourmaline and Fe oxide minerals in nodule tourmaline.

## PETROGRAPHY

### Granite intrusion

Laleh Zar intrusion consists of a variety of intrusive rock types such as diorite, granodiorite, and granite. Granite intrusion shows a fine- to medium-grained leucocratic rocks, with granular and granophyric textures (Figure 2 a,b). Their main minerals are of quartz, K-feldspar, plagioclase and biotite (Figure 2a), tourmaline, zircon, and apatite as accessory minerals. Chlorite, epidote, and sericite are alteration minerals as K-feldspar and plagioclase are often altered into sericite, biotite is altered into chlorite, and plagioclase is altered into epidote. Quartz is anhedral and has a granophyric texture and develops between quartz and large K-feldspar

crystals (intergrowth of quartz and K-feldspar) (Figure 2b). Tourmaline is another minor mineral in these units that is generally black in the hand sample. Based on the tourmaline petrography, several distinct morphology types of tourmaline have been identified. For example: nodule tourmaline, tourmaline-enriched veins, and radial tourmaline that their petrographic characteristics are described below.

### Nodule tourmaline

Nodule tourmaline mainly occurs in the marginal areas of granite intrusion. Some nodules are surrounded by a fine-grained leucocratic zone (halo) (Figure 2c). The nodules are typically round or have an irregular shape with sizes from 2

to 5 cm and the nodules sizes become larger by moving away from the marginal areas of granite intrusion. The nodules consist of tourmaline, quartz, plagioclase, and K-feldspar as main minerals, and epidote and opaque minerals as alteration minerals. Epidote and opaque minerals occur near the tourmaline minerals and some opaque minerals grow on tourmalines (Figure 2f). Tourmaline can be found in a triangular shape and as columnar euhedral crystals (Figure 2 d,e). The contact point between tourmaline and other minerals is planar. The tourmalines show brownish-green pleochroism and its triangular crystals have zoning

colors. The leucocratic halos of the nodules are mainly comprised of quartz and K-feldspar.

#### Radial tourmaline

Radial tourmaline is related to nodule tourmaline and these can be found around the nodule tourmaline (Figure 3a). These consist of tourmaline, quartz and feldspar minerals, and they show granular textures. The radial tourmalines have brown and green colors and are anhedral and subhedral in form (Figure 3b). Tourmaline is between quartz and feldspar as interstitial.

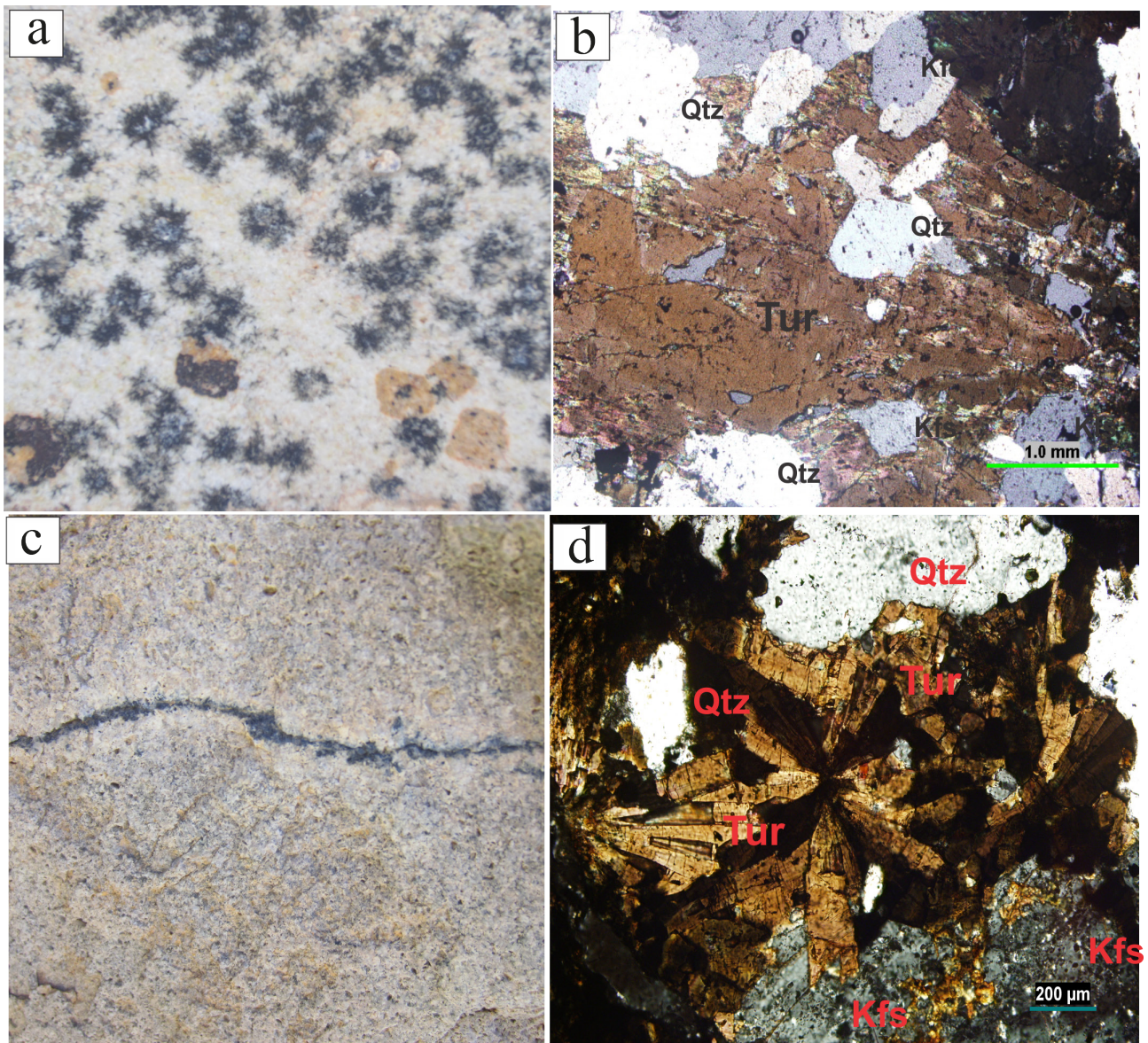


Figure 3. a) Radial tourmaline in leleh Zar granite. b) Microscope image of tourmaline brown color in radial tourmaline (PPL). c) Vein tourmaline in leleh Zar granite. d) Microscope image of brown tourmaline with radial growth in vein tourmaline (XPL), quartz (Qtz), alkali feldspar (Kfs) and tourmaline (Tur).

### Vein tourmaline

The vein tourmaline has different thicknesses ranging from millimeters to centimeters (Figure 3c) that are dispersed in granite and have a fine-grained leucocratic zone (halo). Vein tourmaline is fine- to medium-grained and has granular to perthite textures. They are mainly comprised of quartz, feldspar, tourmaline, and biotite crystals, and biotite is altered into chlorite. Tourmaline is among other minerals as interstitial. Tourmaline in veins occurs mostly as euhedral to subhedral with brownish green pleochroism. Vein tourmaline has needle crystals that grows outward in a spherulitic manner from the center of nucleation (Figure 3d).

### GEOCHEMISTRY OF TOURMALINE

Some results of EPMA of the tourmalines are shown in Table 1. The tourmaline samples showed variations including: 9.28 to 19.14 wt% FeO, 4.06 to 8.28 wt% MgO, 0.01 to 0.15% MnO, 0.11 to 2.10 wt% TiO<sub>2</sub>, 0.46 to 2.01

wt% CaO, 1.79 to 2.63 wt% Na<sub>2</sub>O, 20.82 to 32.32 wt% Al<sub>2</sub>O<sub>3</sub>, and 0.02 to 0.13 wt% K<sub>2</sub>O. The three types of tourmalines show different chemical compositions. Radial and nodule tourmalines have Mg contents higher than vein tourmalines so that the Mg/(Mg+Fe) ratios in radial tourmaline, nodule tourmaline, and vein tourmaline are in a range of 0.37 to 0.53 (with an average of 0.44), 0.36 to 0.59 (with an average of 0.47), and 0.30 to 0.46 (with an average of 0.39) respectively, and the Ca/(Ca+Na) ratios in radial tourmaline, nodule tourmaline, and vein tourmaline are in a range of 0.17 to 0.35 (with an average of 0.24), 0.16 to 0.38 (with an average of 0.25), and 0.09 to 0.35 (with an average of 0.25), since in the Mg/(Mg+Fe) vs Ca/(Ca+Na) diagram (Figure 4a), all the tourmalines fall between the schorl-dravite end-members. As a result, nodule tourmaline and radial tourmaline have a dravite composition and vein tourmalines have Mg-rich schorl composition. Based on the X-site occupancy, the three types of tourmaline belong to alkali group tourmaline (Henry et al., 2011), showing a

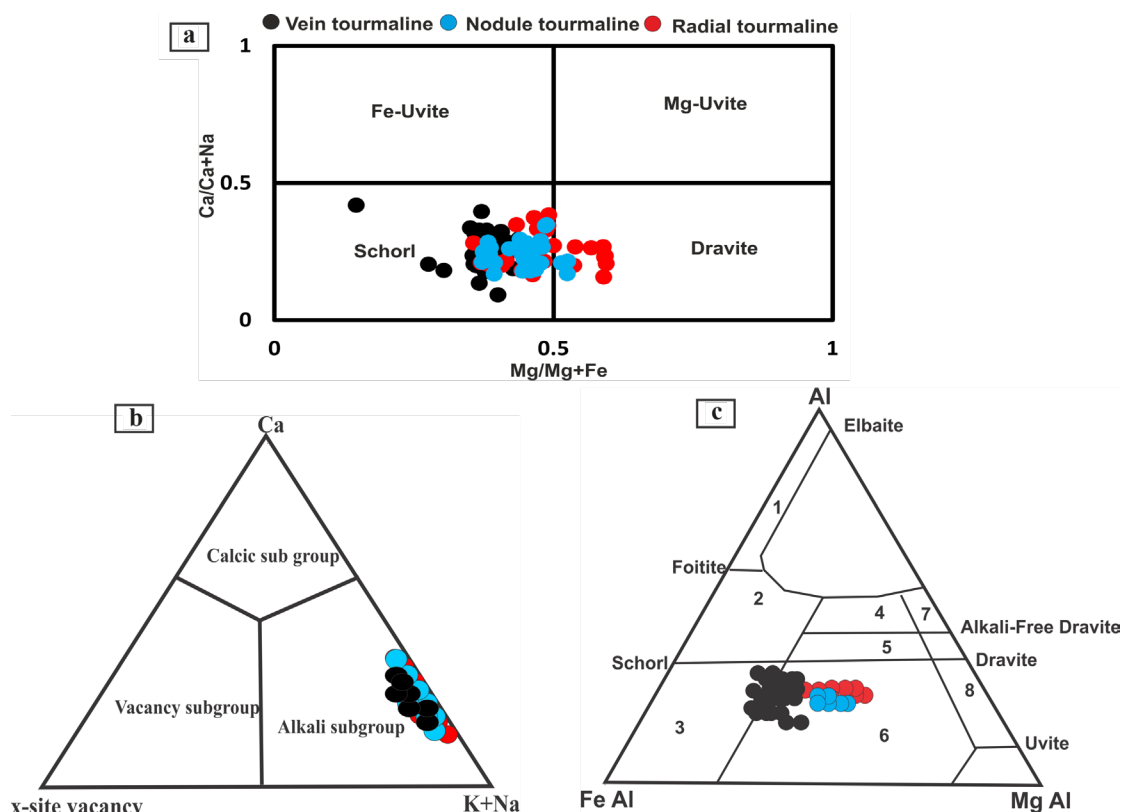


Figure 4. a) Mg/(Mg+Fe) vs Ca/(Ca+Na) diagram. b) Classification of the principal groups of the tourmalines based on the X-site occupancy (Henry et al., 2011). c) Al-Fe(tot)-Mg ternary diagrams (Henry and Guidotti, 1985) (1) Li-rich granitic rocks, pegmatites and aplites, (2) Li poor granitic rocks, pegmatites and aplites, (3) hydrothermally altered granitic rocks, (4) metapelites and metapsammites co-existing with Al-saturating phase, (5) metapelites and metapsammites not co-existing with Al-saturating phase, (6) Fe<sup>3+</sup> rich quartz-tourmaline rocks, calc-silicate rocks and metapelites, (7) Ca-rich metapelites, (8) Ca-poor metapelites, metapsammites and quartz-tourmaline rocks.

trend to the calcic group (Figure 4b). All tourmalines have relatively low Al contents. In detail,  $4.12 < \text{Al}_{\text{tot}} < 6.37$  apfu (with an average of 5.22)  $4.53 < \text{Al}_{\text{tot}} < 6.00$  apfu (with an average of 5.22) and  $4.72 < \text{Al}_{\text{tot}} < 5.40$  apfu (with an average of 5.07) for vein tourmaline, nodule tourmaline, and radial tourmaline (respectively), showing that the Z-site is not fully populated by Al. The values of X-vacancy and Al at the Y site are negligible. The variation of Al content in the three types of tourmaline may be referred to the substitution of Mg and Fe according to the  $(\text{Mg,Fe})(\text{OH})\text{Al}_1\text{O}_{-1}$  exchange vector (Henry and Guidotti, 1985) used to determine the host rock composition; therefore, in the Al-Fe-Mg ternary diagram (Henry and Guidotti, 1985), nodule and radial tourmalines fall under the fields of  $\text{Fe}^{3+}$  rich quartz-tourmaline rocks, calc-silicate rocks, and metapelites, whereas vein tourmalines are in the fields of  $\text{Fe}^{3+}$  rich quartz-tourmaline rocks, calc-silicate rocks, and metapelites and hydrothermally altered granitic rocks (Figure 4c).

### Mechanisms of substitution

Based on the Fe vs Mg plot (Figure 5a), the studied

tourmalines are above the line  $\Sigma(\text{Fe}+\text{Mg})=3$  apfu, indicating that the Al substitution at the Y site is insignificant. It is also observed that there are different correlations between Fe and Mg in the three types of tourmaline: there is positive correlation between Fe and Mg consistent with the substitution  $(\text{Mg,Fe})(\text{OH})\text{Al}_1\text{O}_{-1}$ , while in nodule and radial tourmalines there is an inverse correlation between Fe and Mg, indicating the substitution  $\text{FeMg}_{-1}$ . The diagram of Ca vs Na (Figure 5b) shows that all samples contain  $\text{Ca} > 0.20$  apfu. Therefore, this diagram shows amounts of uvitic component according to the  $\text{CaMgNa}_{-1}\text{Al}_1$  and  $2\text{Ca}_{-1}\text{Na}_{-1}$  exchange vectors. In the Li-Na vs  $\text{Fe}_{\text{tot}}$  diagram (Figure 5c), all tourmalines fall between the  $\text{FeAl}_1$  and  $\text{R}^{2+}(\text{OH})\text{Al}_1\text{O}_{-1}$  exchange vector (where  $\text{R}^{2+} = \text{Fe}^{2+} + \text{Mg}^{2+} + \text{Mn}^{2+}$ ). In the diagram of  $\text{R1}+\text{R2}$  vs  $\text{R3}$  (Figure 5d), all the tourmalines show a proton-loss substitution with  $(\text{Mg,Fe})(\text{OH})\text{Al}_1\text{O}_{-1}$  exchange vector also with an increased Ca-component according to the  $\text{Ca}(\text{MgFe})\text{Na}_{-1}\text{Al}_1$  exchange vector.

### Major element variations and zoning

The BSE images do not show a high variability in zoning

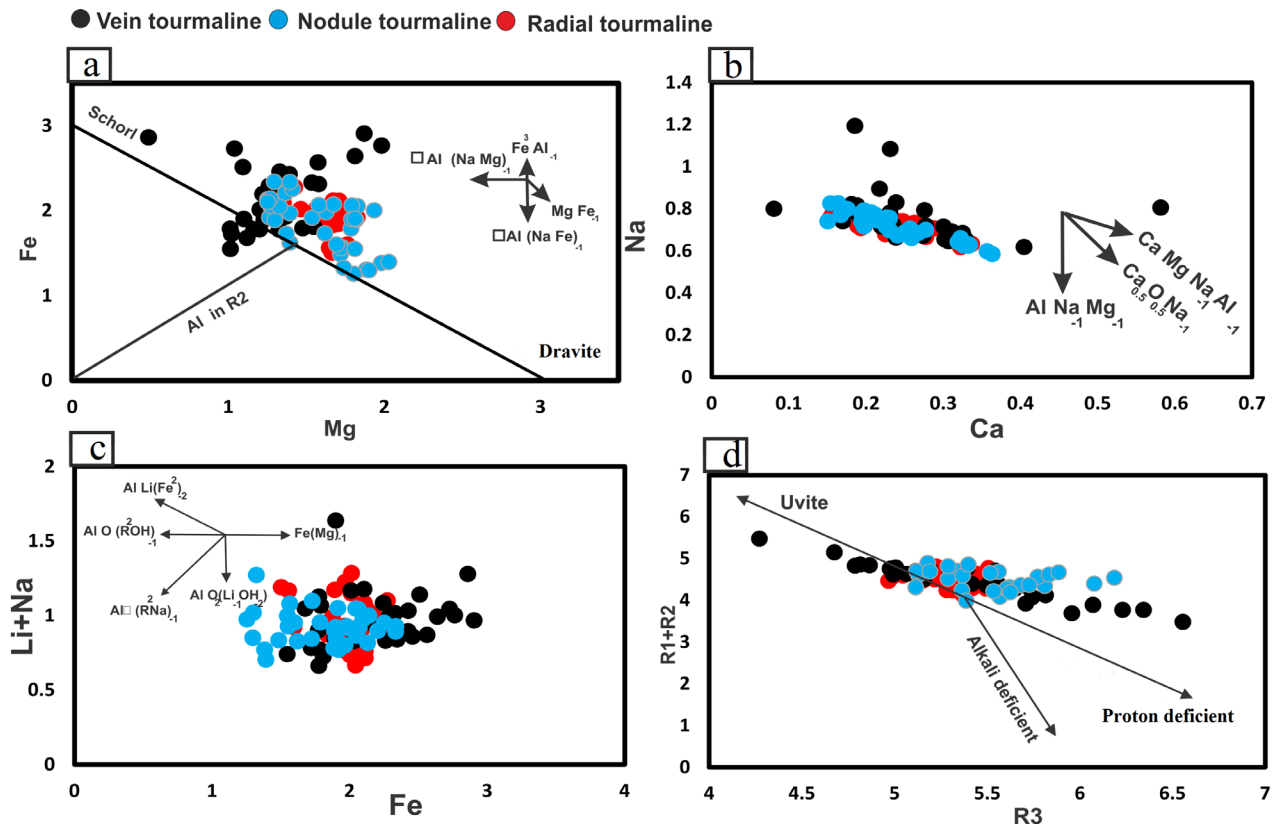


Figure 5. a) Mg vs Fe diagram for tourmalines. b) Ca vs Na diagram showing negative correlation between them. c) Fe(tot) vs (Li+Na). Note that the  $\text{R}^{2+} = \text{Fe}^{2+} + \text{Mg}^{2+} + \text{Mn}^{2+}$ . d) Diagram of  $(\text{R1}+\text{R2})$  vs  $\text{R3}$ .

for the studied tourmalines except for nodule tourmaline that is heterogeneous showing oscillatory to patchy zoning (Figure 6a). The nodule and radial tourmalines have inclusions of K-feldspar mineral. Vein and radial tourmalines are homogeneous (Figure 6 b,c). Longfellow and Swanson (2011) suggested that homogeneous tourmaline crystals are probably crystallized from a granitic melt. These facts indicate that the mineral assemblages of all morphological types of tourmaline are very simple and include feldspar and quartz. The zonation is described in terms of ratios of substituting cations and ratios of major element concentrations. The optical zonation of nodule tourmaline correlates with variations in the chemical composition of the core and rim zones in a way that from the core to rime of nodule tourmaline crystals increase the concentration of Ti, Fe, Mn, and Na and decrease the concentration of Al, Ca, and Mg (Figure 7). Black (1971), Fortey and Cooper (1986), and Slack and Coad (1989) stated that the brown color of tourmaline can be attributed to enrichment in Ti. Longfellow and Swanson (2011), stated that color zoning in a varieties of tourmaline are attributed to a wide variation in Ti, as low Ti correlates with blue

tourmaline and high Ti correlates with brown tourmaline; therefore, this optically complex zonation pattern, yet a weak chemical variation, is indicative of magmatic origin. From core to rime in the radial tourmaline, the concentration of Al, Ti, Mg, and Na is increased and the concentration of Ca, Fe, and Mn is decreased; and from core to rime in vein tourmaline, the concentration of Al, Mn, and Na is increased and the concentration of Ti, Mg, and Ca is decreased (Figure 7). This shows that different types of tourmaline have different chemical variations. Van Hinsberg et al. (2006) suggested that chemical differences between core and rime zones may indicate a change in the chemical composition of the melt or the transition of the magmatic to a fluid-controlled stage. The blue tourmaline has lower amounts of Ti, Fe, and Ca than the brown tourmaline and this pattern can be the result of tourmaline formation in late-stage fractionation of magma. The variation in color (brown and green in most tourmalines) may be associated with variation in Ti and Fe. Dutrow and Henry (2000) suggested that different compositions in a tourmaline are the result of a change in fluid composition during the growth of tourmaline crystal. Von Goerne et al. (2001) stated that the Na content

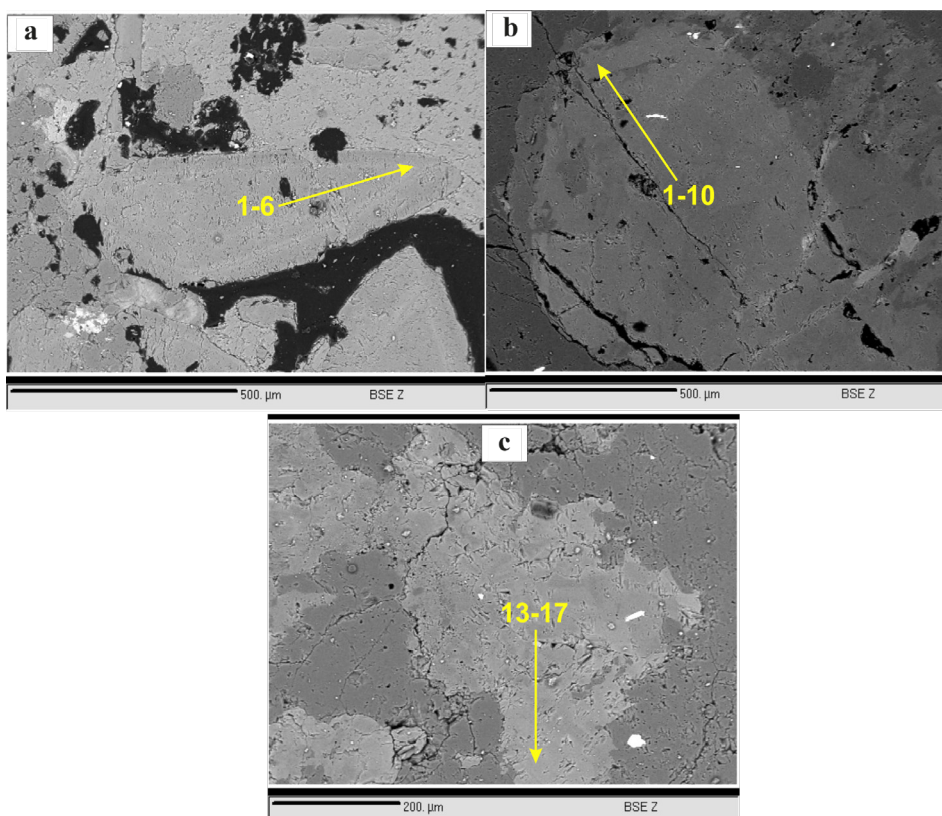


Figure 6. Back-scattered electron (BSE) images of a) Nodule tourmaline with week zoning. b) Radial tourmaline with homogeneous crystal. c) Vein tourmaline with homogeneous crystal.

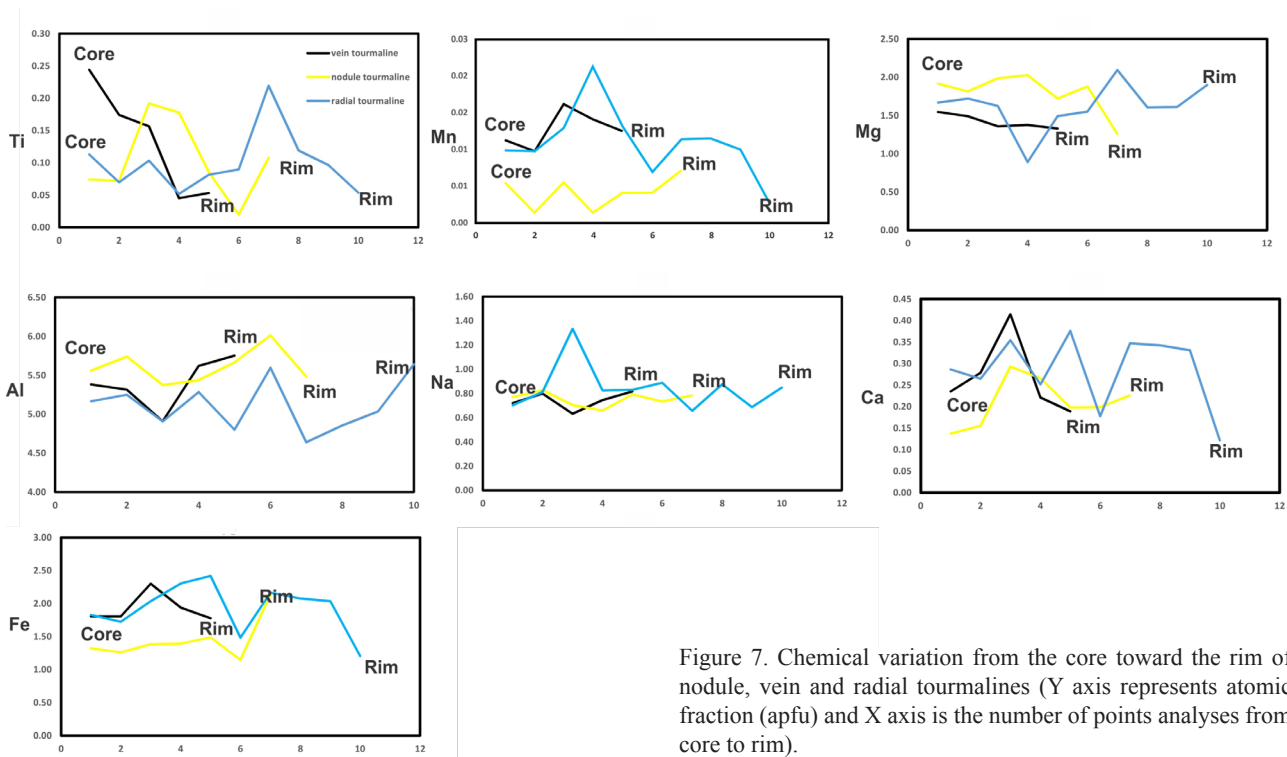


Figure 7. Chemical variation from the core toward the rim of nodule, vein and radial tourmalines (Y axis represents atomic fraction (apfu) and X axis is the number of points analyses from core to rim).

increases with increasing temperature in tourmaline, but the Na content of the fluid could be more important than temperature in controlling the incorporation of Na in the structure. At lower Na contents of fluid, the Na content of tourmaline increases with increasing temperature, but at higher Na contents of fluid, the converse is true (Von Goerne et al., 2001).

## DISCUSSION

Laleh Zar granitoid batholith consists of granite to granodiorite compositions. Tourmalinization is restricted to granitic rock and has low abundance. This shows that granitic magma has been under saturation in B element. In this granite, there are tourmalines in forms of nodule, radial, and vein. The nodule tourmalines are euhedral and there is not any textural evidence that they have replaced pre-existing phases. In contrast, there is micro feldspar crystal in tourmaline as inclusion, indicating that nodule tourmaline is crystallized after the crystallization of K-feldspar. Radial tourmaline can be found around nodule tourmaline. Nodule and radial tourmalines have Mg-rich schorl to dravite compositions, with Al<6 apfu and no vacancy at the X site; nodule tourmaline shows optical and chemical zonation, while radial tourmaline do not such a zonation. Vein tourmaline has a schorl composition, with Al<6 apfu and no vacancy at the X site and does not show zonation. Benard et al. (1985) showed

that magmatic tourmaline has high amounts of Fe/Mg ratios, F, Al, and vacancy at the X site, but hydrothermal tourmaline exhibits zonation and is rich in Mg. Moreover, the tourmaline formed from hydrothermal fluids shows fine-scale oscillatory-type zonation (Samson and Sinclair, 1992; London and Manning, 1995). Magmatic tourmaline generally has little or none optical zonation (Manning, 1982; London and Manning, 1995). Grew (2002) suggested that concentrations of Al, Mn, and Fe/(Fe+Mg) increase during differentiation. The nodule and radial tourmalines have Na/(Na+Ca) ratios close to the vein tourmalines, but have higher and variable Mg/(Fe+Mg) ratios. Vein tourmaline has needle crystals that grow outward from the center of nucleation in a spherulitic manner; this directed growth is consistent with crystallization from magma with a compositional and thermal gradient (London, 2008). All tourmalines have chemical zonation including significant fluctuations in Al, Fe, Mg, Na, Ca, and Ti. This chemical variability can be attributed to changes in fluid composition during tourmaline crystallization as stated by Dutrow and Henry (2000) and Van Hinsberg et al. (2006), who also pointed out that they are a result of changes in fluid compositions during the growth of tourmaline crystal. Based on the substitution diagram,  $\text{Ca}(\text{Mg,Fe})\text{Na}_{-1}\text{Al}_{-1}$ ,  $(\text{Fe,Mg})(\text{OH})\text{Al}_{-1}\text{O}_{-1}$ , and  $\text{MgFe}_{-1}$  exchange vectors are dominant substitutions in all studied tourmalines. Based on Al, Fe, and Mg contents,

all tourmalines are within the range of Fe<sup>3+</sup>-rich quartz-tourmaline rocks, metapelites, and calc-silicate rocks, but radial tourmaline has a tendency toward metapelites and metapsammities that do not co-exist with the Al-saturated phase. On the other hand, Niktabar et al. (2015) concluded that Laleh Zar batholith is type I and is the result of lower continental crust melting, contaminated with upper continental crust during its evolution and placement. Thus, B, H<sub>2</sub>O and Al contents of magma are increased due to being contaminated with upper continental crust, while B can be the result of melting of metasedimentary rocks in the upper crust. Experimental and field studies (Veksler and Thomas, 2002; Veksler, 2004) have shown that hydrous, B-rich melts are enriched with B, Na, and Fe and are immiscible in aluminosilicate melts. In addition, tourmalines in granite-related hydrothermal systems with FeO/(FeO+MgO) ratio lower than 0.6 would suggest that fluids have moved across a long distance in an exo-granitic, commonly sediment-hosted setting (Pirajno and Smithies, 1992). However, all the tourmalines in Laleh Zar granite are endo granite and have FeO/(FeO+MgO) ratio 0.62 to 0.75, 0.68 to 0.80 and 0.55 to 0.76 for radial, vein and nodule tourmalines and ratios lower than 0.6 for nodule tourmaline, which can be due to the mixing of juvenile fluids and volatiles coming from evolved granitic magma. Jiang (2015) has studied the different types of nodule tourmaline from the Nyalam leucogranites, South Tibetan Himalaya, showing that the origin of tourmaline nodules is related to different stages of syn-magmatic crystallization from a B-rich melt, or the subsequent transition from magmatic to hydrothermal environment, or crystallization in post-magmatic hydrothermal fluids. Jiang et al. (2003) has also studied the tourmalines of Lavicky leucogranite, showing that quartz-tourmaline orbicules is Fe-rich schorl and quartz-tourmaline veins is Mg-rich dravite. He concluded that quartz-tourmaline orbicular has been formed during a transition from magmatic to hydrothermal processes, whereas the vein tourmalines have been formed from mixing of exsolved magmatic-hydrothermal fluids with an external fluid rich in Ca and Mg. Mineral chemistry of the nodule tourmaline is similar to those described for nodule tourmaline from Cape Granite Suite, South Africa (Rozendaal and Bruwer, 1995), and the mineral chemistry of radial and nodule tourmalines are similar to those described for tourmaline nodules from the Lavicky leucogranite (Tg-I and Tg-II type tourmalines, respectively). There are epidote and opaque minerals in nodule tourmaline as alteration minerals, whereas radial tourmalines that exist around nodule tourmalines do not contain these minerals. Based on petrographic and chemical characteristics of tourmalines, vein tourmaline has been formed during a transition from magmatic to hydrothermal processes

and radial tourmaline has been formed by mixing of magmatic-hydrothermal fluids with an external fluid rich in Ca and Mg; whereas nodule tourmaline is probably the result of post-magmatic hydrothermal environment with the influence of an external fluid that for example, could have come from the wall rocks.

## CONCLUSION

Laleh Zar granitoid batholith is type I with granite to granodiorite composition that is the result of melting of the lower continental crust. Tourmalinization is restricted to granitic rocks and has low abundance. This indicates that granitic magma has been under saturation in B element. Since granitic magma has been contaminated by the upper continental crust during its evolution and placement, B, H<sub>2</sub>O, and Al content of magma are increased via contamination with the upper continental crust and with metasedimentary rocks. This granite contains tourmalines in the form of nodule, radial, and vein. Microprobe analyses have revealed that the studied tourmalines correspond to schorl and dravite. Nodule and radial tourmalines have Mg-rich schorl to dravite compositions, with Al<6 apfu no vacancy at the X site. Nodule tourmaline shows optical and chemical zonation, whereas radial tourmaline does not show optical zoning. Vein tourmaline has a schorl composition, with Al<6 apfu and no vacancy at the X site as well as no optical zoning. Ca(Mg,Fe)Na<sub>1</sub>Al<sub>1</sub>, (Fe,Mg)(OH)Al<sub>1</sub>O<sub>1</sub> and MgFe<sub>1</sub> exchange vectors are dominant substitutions in of the studied tourmalines. These substitutions can be ascribed to changes in fluid composition during tourmaline crystallization. The chemical zoning patterns found in tourmalines include significant fluctuations in Al, Fe, Mg, Na, Ca, and Ti; brown and green tourmalines are the result of changes in Ti and Fe. Based on the petrographic and chemical characteristics of tourmalines, it can be concluded that: (1) vein tourmaline has been formed during a transition from magmatic to hydrothermal processes; (2) radial tourmaline has been formed by mixing of magmatic-hydrothermal fluids with an external fluid rich in Ca and Mg; (3) nodule tourmaline is probably the result of post-magmatic hydrothermal environment through the influence of an external fluid coming from the wall rocks of the nodule.

## ACKNOWLEDGEMENTS

We thank from the financial support of Lorestan University. Also, the authors thank the editor and reviewers for their valuable comments and suggestions that improved the manuscript significantly.

## REFERENCES

- Agard P., Omrani J., Jolivet L., Mouthereau F., 2005. Convergence history across Zagros, Iran: constraints from collisional and earlier deformation. *International Journal of Earth Sciences* 94, 401-419.
- Ahmadian J., Haschke M., McDonald I., Regelous M., Ghorbani M., Emami M., Murata M., 2009. High magmatic flux during Alpine-Himalayan collision: Constraints from the Kal-e-Kafi complex, central Iran. *Geological Society of America Bulletin* 121, 857-868.
- Balen D. and Broska I., 2011. Tourmaline nodules: products of devolatilization within, the final evolutionary stage of granitic melt? *Geological Society London Special Publications* 350, 53-68.
- Benard F., Moutou P., Pichavant M., 1985. Phase relations of tourmaline leucogranites and the significance of tourmaline in silicic magmas. *The Journal of Geology* 93, 271-291.
- Black P.M., 1971. Tourmalines from Cuvier Island, New Zealand. *Mineralogical Magazine* 38, 374-376.
- Bosi F., 2018. Tourmaline crystal chemistry. *American Mineralogist* 103, 298-306.
- Dimitrijevic M.D., 1973. Geology of Kerman Region. Geological Survey of Iran, Report Number Yu/52, 334 pp.
- Dutrow B.L. and Henry D.J., 2000. Complexly zoned fibrous tourmaline, Cruzeiro mine, Minas Gerais, Brazil: a record of evolving magmatic and hydrothermal fluids. *Canadian Mineralogist* 38, 131-143.
- Fortey N.J. and Cooper D.C., 1986. Tourmalinization in the Skiddaw Group around Crummock Water, English Lake District. *Mineralogical Magazine* 50, 17-26.
- Grew E.S., 2002. Borosilicates (exclusive of tourmaline) and boron in rock-forming minerals in metamorphic environments. In *Boron: Mineralogy, Petrology and Geochemistry*, 2<sup>nd</sup> printing (E.S. Grew and L.M. Anovitz, Eds.). *Reviews in Mineralogy* 33, 387-502.
- Guiraud R. and Bosworth W., 1997. Senonian basin inversion and rejuvenation of rifting in Africa and Arabia: synthesis and implications to plate-scale tectonics. *Tectonophysics* 282, 39-82.
- Hassanzadeh J., 1993. Metallogenic and tectonomagmatic event in the SE sector of Cenozoic active continental margin of Central Iran (Shahre Babak area), Kerman Province. Ph.D. thesis, California, Los Angeles, 204 pp.
- Hawthorne F.C. and Henry D.J., 1999. Classification of minerals of tourmaline group. *European Journal of Mineralogy* 11, 201-215.
- Henry D.J. and Guidotti C.V., 1985. Tourmaline as a petrogenetic indicator mineral: an example from the staurolite-grade metapelites of NW Maine. *American Mineralogist* 70, 1-15.
- Henry D.J., Novak M., Hawthorne, F.C., Ertl A., Dutrow B., Uher P., Pezzotta F., 2011. Nomenclature of the tourmaline supergroup-minerals. *American Mineralogist* 96, 895-913.
- Hou Z.Q., Zhang H., Pan X., Yang Z., 2011. Porphyry Cu (-Mo-Au) deposits related to melting of thickened mafic lower crust: Examples from the eastern Tethyan metallogenic domain. *Ore Geology Reviews* 39, 21-45.
- Jiang S.Y., Yang J.H., Novak M., Selway J.B., 2003. Chemical and boron isotopic compositions of tourmaline from the Lavicky leucogranite, Czech Republic. *Geochemical Journal* 37, 545-556.
- Jiang S.Y., 2015. Chemical and boron isotopic compositions of tourmaline from the Nyalam leucogranites, South Tibetan Himalaya. *Chemical Geology* 419, 102-113.
- Kirkham R.V. and Dunne K.P., 2000. World distribution of porphyry, porphyry-associated skarn, and bulk-tonnage epithermal deposits and occurrences. *Geological Survey of Canada, Open File* 3792-26.
- London D. and Maning D.A.C., 1995. Chemical variation and significance of tourmaline from SW England. *Economic Geology* 90, 495-519.
- London D., 2008. Pegmatites. *The Canadian Mineralogist, Special Publication* 10, 347 p.
- Longfellow K.M. and Swanson S.E., 2011. Skeletal tourmaline, undercooling, and crystallization history of the Stone Mountain granite, Georgia, U.S.A. *Canadian Mineralogist* 49, 341-357.
- Manning D.A.C., 1982. Chemical and morphological variation in tourmalines from the Hub Kapong batholith of granites in peninsular Thailand. *Mineralogical Magazine* 45, 139-147.
- McClay K.R., Whitehouse P.S., Dooley T., Richards M., 2004. 3D evolution of fold and thrust belts formed by oblique convergence. *Marine Geology* 21, 857-877.
- McInnes B., Evans N.J., Fu F.Q., Garwin S., 2005. Application of thermochronology to hydrothermal ore deposits. *Reviews in Mineralogy and Geochemistry* 58, 467-498.
- Mohajjel M., Fergusson C.L., Sahandi M.R., 2003. Cretaceous-Tertiary convergence and continental collision, Sanandaj-Sirjan zone, western Iran. *Journal of Asian Earth Sciences* 21, 397-412.
- Niktabar M., Moradian A., Ahmadipour H., 2015. Investigation of Mineralogy and Granitoid Geochemistry in Laleh Zar Region (Bardsir - Kerman Province). *Iranian Journal of Crystallography and Mineralogy* 4, 803-818.
- Palmer M.R. and Slack J.F., 1989. Boron isotopic composition of tourmaline from massive sulphide deposits and tourmalinites. *Contributions to Mineralogy and Petrology* 103, 434-451.
- Perugini D. and Poli G., 2007. Tourmaline nodules from Capo Bianco aplite (Elba Island, Italy) an example of diffusion limited aggregation growth in a magmatic system. *Contributions to Mineralogy and Petrology* 153, 493-508.
- Pirajno F. and Smithies R.H., 1992. The FeO/(FeO+MgO) ratio of tourmaline: A useful indicator of spatial variations in granite-related hydrothermal mineral deposits. *Journal of Geochemical Exploration* 42, 371-381.
- Razique A., Lo Grasso G., Livesey T., 2007. Porphyry copper-gold deposits at Reko Diq complex, Chagai Hills Pakistan. *Proceedings of Ninth Biennial SGA Meeting, Dublin*.

- Richards J.P., 2012. Post subduction porphyry Cu-Au and epithermal Au deposits: products of remelting of subduction-modified lithosphere. *Geology* 37, 247-250.
- Rozendaal A. and Bruwer L., 1995. Tourmaline nodules indicator of hydrothermal alteration and Sn-Zn-(W) mineralization in the Cape Granite Suite, South Africa. *The Journal of African Earth Sciences* 21, 141-155.
- Samson I.M. and Sinclair W.D., 1992. Magmatic hydrothermal fluids and the origin of quartz-tourmaline orbicules in the Seagull Batholith, Yukon Territory. *Canadian Mineralogist* 30, 937-954.
- Shafei B., Shahabpour J., Haschke M., 2008. Transition from Paleogene normal calc-alkaline to Neogene adakitic-like plutonism and Cu-metallogeny in the Kerman porphyry copper belt: response to Neogene crustal thickening. *Journal of Sciences, Islamic Republic of Iran* 19, 67-84.
- Shafei B., Haschke M., Shahabpour J., 2009. Recycling of orogenic arc crust triggers porphyry Cu mineralization in Kerman Cenozoic arc rocks, southeastern Iran. *Mineralium Deposita* 44, 265-283.
- Slack J.F. and Coad P.R., 1989. Multiple hydrothermal and metamorphic events in the Kidd Creek volcanogenic massive sulphide deposit, Timmins, Ontario: evidence from tourmalines and chlorites. *Canadian Journal of Earth Sciences* 26, 694-715.
- Trumbull R.B., Krienitz M.S., Gottesmann B., Wiedenbeck M., 2008. Chemical and boron-isotope variations in tourmalines from an S-type granite and its source rocks: the Erongo granite and tourmalinites in the Damara Belt, Namibia. *Contributions to Mineralogy and Petrology* 155, 1-18.
- Van Hinsberg V.J., Schumacher J.C., Kearns S., Mason P.R.D., Franz G., 2006. Hourglass sector zoning in metamorphic tourmaline and resultant major and trace-element fractionation. *American Mineralogist* 91, 717-728.
- Veksler I.V. and Thomas R., 2002. An experimental study of B-, P- and Frich synthetic granite pegmatite at 0.1 and 0.2 GPa. *Contributions to Mineralogy and Petrology* 143, 673-683.
- Veksler I.V., 2004. Liquid immiscibility and its role at the magmatic hydrothermal transition: a summary of experimental studies. *Chemical Geology* 210, 7-31.
- Von Goerne G., Franz G., Heinrich W., 2001. Synthesis of tourmaline solid solutions in the system  $\text{Na}_2\text{O}-\text{MgO}-\text{Al}_2\text{O}_3-\text{SiO}_2-\text{B}_2\text{O}_3-\text{H}_2\text{O}-\text{HCl}$  and the distribution of Na between tourmaline and fluid at 300 to 700 °C and 200 MPa. *Contributions to Mineralogy and Petrology* 141, 160-173.
- Xavier R.P., Wiedenbeck M., Trumbull R.B., Dreher A.M., Monteiro L.V.S., Rhede D., de Araujo, and C.E.G., Torresi I., 2008. Tourmaline B-isotopes fingerprint marine evaporates as the source of high-salinity ore fluids in iron oxide copper-gold deposits, Carajas Mineral Province (Brazil). *Geology* 36, 743-746.
- Yang S.Y. and Jiang S.Y., 2012. Chemical and boron isotopic composition of tourmaline in the Xiangshan volcanic-intrusive complex, Southeast China: Evidence for boron mobilization and infiltration during magmatic-hydrothermal processes. *Chemical Geology* 312, 177-189.



This work is licensed under a Creative Commons Attribution 4.0 International License CC BY. To view a copy of this license, visit <http://creativecommons.org/licenses/by/4.0/>

